Atmos. Chem. Phys. Discuss., 8, 6571–6601, 2008
www.atmos-chem-phys-discuss.net/8/6571/2008/

Atmospheric Chemistry and Physics Discussions

Particle size distributions in the Eastern Mediterranean troposphere

N. Kalivitis[1], W. Birmili[2], M. Stock[2,*], B. Wehner[2], A. Massling[2,], A. Wiedensohler[2], E. Gerasopoulos[1,***], and N. Mihalopoulos[1]**

[1]Environmental Chemical Processes Laboratory, Department of Chemistry, University of Crete, Greece
[2]Leibniz-Institute for Tropospheric Research, Leipzig, Germany
[*]now at: Alfred Wegener Institute for Polar and Marine Research, Potsdam, Germany
[**]now at: National Environmental Research Institute, Aarhus University, Roskilde, Denmark
[***]now at: Institute for Environmental Research and Sustainable Development, National Observatory of Athens, Athens, Greece

Received: 26 February 2008 – Accepted: 6 March 2008 – Published: 4 April 2008

Correspondence to: N. Mihalopoulos (mihalo@chemistry.uoc.gr)

Published by Copernicus Publications on behalf of the European Geosciences Union.

Abstract

Atmospheric particle size distributions were measured on Crete island, Greece in the Eastern Mediterranean during an intensive field campaign between 28 August and 20 October 2005. Our instrumentation combined a differential mobility particle sizer (DMPS) and an aerodynamic particle sizer (APS) and measured number size distributions in the size range 0.018 μm–10 μm. Four time periods with distinct aerosol characteristics were discriminated, two corresponding to marine and polluted air masses, respectively. In marine air, the sub-μm size distributions showed two particle modes centered at 67 nm and 195 nm having total number concentrations between 900 and 2000 cm^{-3}. In polluted air masses, the size distributions were mainly unimodal with a mode typically centered at 140 nm, with number concentrations varying between 1800 and 2900 cm^{-3}. Super-μm particles showed number concentrations in the range from 0.01 to 2.5 cm^{-3} without any clear relation to air mass origin. A small number of short-lived particle nucleation events were recorded, where the calculated particle formation rates ranged between 1.1–1.7 cm^{-3} s^{-1}. However, no particle nucleation and growth events comparable to those typical for the continental boundary layer were observed. Particles concentrations (Diameter <50 nm) were low compared to continental boundary layer conditions with an average concentration of 300 cm^{-3}. The production of sulfuric acid and its subsequently condensation on preexisting particles was examined with the use of a simplistic box model. These calculations suggested that the day-time evolution of the Aitken particle population was governed mainly by coagulation and that particle formation was absent during most days.

1 Introduction

During the past decades, atmospheric research has been concerned with the global distribution of atmospheric aerosol particles because of their effects on global climate by interaction with the incoming solar radiation (Haywood and Boucher, 2000; Lohmann

ACPD

8, 6571–6601, 2008

and Feichter, 2005), their oxidation capacity of the atmosphere (Ravishankara, 1997), and their adverse effects on human health (HEI, 2002; WHO, 2004). Aerosols are identified to play a key role on earth radiation budget alleviating Green House Gases (GHGs) effects, it is therefore vital to understand the past and possible future influence of aerosols on regional and global climate (Solomon et al., 2007).

The Mediterranean area is of special interest for global climate research because its atmosphere is influenced likewise by continental and maritime aerosol sources and complex boundary layer processes. Especially for the Eastern Mediterranean area, the dominance of northerly winds during summer leads to transport of polluted air masses from the main continental Europe (e.g. Lelieveld et al., 2002). Moreover, due to its proximity to North Africa, Saharan dust can be frequently observed during the transition periods (e.g. Kalivitis et al., 2007). The combination of solar irradiance with the sea water in the marine environment results in high levels of relative humidity (RH), that causes aerosols to take up water and therefore contribute significantly to direct radiative forcing even in the absence of clouds. Indeed, during July/August 2001, Markowicz et al. (2002) showed that aerosols of anthropogenic origin in the Eastern Mediterranean area, can contribute to a diurnal average reduction of 17.9 $W\,m^{-2}$ in the surface solar radiation, an increase of 11.3 $W\,m^{-2}$ in the atmospheric solar absorption, and an increase of 6.6 $W\,m^{-2}$ in the reflected solar radiation at the top-of-the atmosphere. Moreover, Vrekoussis et al. (2005) deduced radiative forcing estimates at the top of the atmosphere (TOA) in the order of $-10\,W\,m^{-2}$ during the dry period (May to October).

Atmospheric particle number size distributions are among the most important parameters from which the atmospheric effects of an aerosol population can be derived (Penner et al., 1998). Since particle number size distributions can be measured with high time resolution, they can be used to distinguish between different air mass types, as well as to identify particle formation, and possibly transformation and removal processes. In situ observations of particle number size distributions in the Eastern Mediterranean are thus important for evaluation of these processes, however they are

ACPD
8, 6571–6601, 2008

scarce, and have been limited to restricted periods in urban areas (e.g. Petäjä et al., 2007).

To better understand the variability and climatic role of aerosols in Eastern Mediterranean, intensive measurements of atmospheric aerosol particles were conducted between August and October 2005 at a remote location on Crete Island (ARIADNE – **A**er**o**sol Phys**i**cal and Chemic**a**l I**d**e**n**tification on Cr**e**te). The main goals of the ARIADNE field study were to determine representative atmospheric particle number size distributions and analyze them according to their potential source regions. Additional results from the campaign, such as the hygroscopic particle properties and chemical particle composition will be presented in a separate paper.

2 Experimental

2.1 The atmospheric research station Finokalia, Crete

Particle measurements were conducted between 29 August and 20 October 2005 at the Finokalia research station, a remote coastal site in the northeastern part of the island of Crete, Greece (35°20′ N, 25°40′ E). Heraklion, the largest city on Crete with a population of about 140.000 inhabitants can be found 70 km east of Finokalia. A major urban agglomeration on the northern shore of the Mediterranean is Athens (~4.5 Mio. inhabitants), located about 350 km northwest of the station. Athens and other urban centers of continental Europe and Asia are the main sources of pollution transported over eastern Mediterranean, mainly in summer when N-NW winds prevail (Gerasopoulos et al., 2005). A detailed description of the measurement site and the prevailing meteorology has been given by Mihalopoulos et al. (1997). Further details on the current operations at Finokalia can be found on http://finokalia.chemistry.uoc.gr.

ACPD
8, 6571–6601, 2008

2.2 Particle number size distributions measurements

Ambient particle number size distributions were measured using a flow-controlled differential mobility particle sizer (DMPS). This instrument follows the general design described in Birmili et al. (1999). Briefly, the instrument consisted of a differential mobility analyzer (DMA; Vienna type, cf. Winklmayr et al., 1991), combined with a condensation particle counter (model 3010, TSI Inc., St. Paul). The system scanned across a particle size range between 18 and 800 nm. Sheath air was circulated in a closed loop and maintained at relative humidities between 10 and 30%. The aerosol inlet was equipped with an Andersen PM_{10} sampling head. Because of the high absolute humidity present in ambient air, aerosol samples were dried before mobility analysis in a diffusion drier based on the Nafion^{TM} membrane technology (Perma Pure LLC Inc., Toms River, USA). This drying step was crucial because the laboratory container at Finokalia was air-conditioned with temperature control at 22°C, so that in the case of significantly higher ambient temperatures to avoid water condensation in the aerosol lines entering the container. Based on laboratory calibrations, the effect of particle losses during the passage of aerosol through the diffusion drier can be neglected for the size range 18–800 nm where the DMPS system was operated.

In addition to the DMPS, coarse particle number size distributions were measured across an aerodynamic particle size range between 0.8 and 10 μm using an aerodynamic particle sizer (APS; model 3321, TSI Inc., St Paul, USA; see Peters and Leith, 2003).

2.3 Additional aerosol measurements

During ARIADNE concurrent measurements were carried out in order to fully characterize the physico-chemical properties of atmospheric particles in the area of Eastern Mediterranean. Scattering coefficient of aerosol particles was recorded using a TSI model 3563 nephelometer at three wavelengths, 450, 550 and 700 nm. Additionally, the effect of hygroscopic growth of aerosols on light scattering was estimated by

measuring the scattering coefficient at 532 nm with two nephelometers (Radiance Research, model M903) in a row, using a drier in between. The absorption coefficient was measured at 670 nm with a Multi Angle Absorption Photometer (MAAP, model 5012), at 330 and 880 nm with a Magee Scientific Aethalometer and at 565 nm with a Particle Soot Absorption Photometer (PSAP, model Radiance Research).

PM_{10} particulate matter was monitored using an Eberline FH 62 I-R Particulate monitor and ozone concentration was measured continuously by a Thermo Electron 49C. Finally, regular sampling of TSP using filters and PM_{10} Small Deposit area low pressure Impactor sampling (SDI; Maenhaut et al., 1996) was provided to determine the chemical composition of the observed atmospheric particles. The identification of the wind direction and air mass origin was based on 5-day back-trajectories calculated by the HYSPLIT model (Hybrid Single-Particle Lagrangian Integrated Trajectory Model; Draxler and Hess, 1998).

3 Observations

3.1 Particle number concentrations

The total particle number concentration at Finokalia station for the period 28 August–20 October 2005 is shown in Fig. 1a. Three frequency ranges of variability were evident: the low-frequency variability demonstrating the reduction of particle number from late summer to autumn, the mid-frequency variability in the order of few days, possibly corresponding to different synoptic conditions and air mass origins, and finally the high-frequency variability represented as short-duration, episodical spikes.

The influence from air masses with different characteristics is examined with back trajectory analysis using the HYSPLIT model. Throughout the whole period air masses from the wide NW-NE sector prevailed (83% of the period), indicating influence from continental Europe sources. During the rest of the days air masses originated either from W or SW. The average total particle number concentration was about 1800 cm^{-3},

ACPD
8, 6571–6601, 2008

the maximum was 4560 cm^{-3} and the minimum was 360 cm^{-3}, the latter being typical for remote coastal areas (Seinfeld and Pandis, 1998). During the first period of the field study (28 August–8 September) air masses from industrialized areas over Turkey, Eastern and Western Europe resulted to high aerosol loading over Finokalia station. On 9 September, particle number concentrations started gradually decreasing and henceforth lower levels of concentrations were established with observed elevations mainly due to certain episodes.

During this study, four periods were distinguished by different levels of total particle number concentration, which also corresponded to different air mass origins: Period A (21–25 September) represents air masses originating over Western Mediterranean (Fig. 2a), with particle number concentrations ranging between 900–1200 cm^{-3} (interquartile range), and thus this period corresponds to maritime aerosols. During period B (27–30 September) northerlies prevailed, introducing pollution aerosols from continental Greece and Eastern Europe (Fig. 2b), resulting in elevated particle loadings (2300–2900 cm^{-3}). During period C (1–4 October) maritime aerosols enriched with pollution from Western Europe, leaded to intermediate concentrations in the range of 1200–2000 cm^{-3}. Finally, period D (5–12 October) was influenced by continental air masses arriving from Turkey and the Black Sea, resulting in total particle number concentrations of 1800–2500 cm^{-3}. The above defined periods will be used for identifying average distributions accounting for different types of air masses. Representative particle number concentration values for each period are summarized in Table 1.

To understand the variability of total particle number concentrations, particle number time series for different size ranges are plotted in Fig. 1b. We have discriminated between the following size ranges: Young Aitken (18–50 nm), Aitken (50–100 nm), accumulation (100–1000 nm) and coarse (1–10 μm). On average, half of total particle number was derived from the accumulation mode, one third lied in the Aitken mode and the rest were Young Aitken mode particles. Coarse particles were limited in number, however when reaching their maximum concentration, they can be a significant portion of the total particle volume and particle mass as discussed later. The low frequency

variability of the total particle number concentrations was controlled by both Aitken and accumulation modes, indicating the equally significant role of the regional/local sources and transported particles during this period.

The accumulation mode, corresponding to transported pollution aerosols, is mainly responsible for the mid-frequency variability e.g. 11–14 and 27–30 September 2005. Finally, a certain number of spikes were related with new particle formation as can be seen in the Young Aitken mode (Fig. 1b). These spikes are evident when very low number concentrations of accumulation mode particles are observed, especially when maritime air masses prevailed, such as periods A and C of Fig. 1a. Since accumulation particles are limited in number, precursor gases are not scavenged onto preexisting particles and formation of new particles is possible as discussed in Sect. 3.3.

3.2 Particle size distributions

3.2.1 Air-mass specific size distributions

Apart from the particle number concentrations, number size distributions were additionally examined. The mean diurnal evolution of the number size distributions for each of the distinguished periods A, B, C and D of Fig. 1 are presented in Fig. 3. Two typical size distributions were found during the period under study, characteristically for background and polluted conditions respectively (Fig. 4). During the prevalence of maritime air masses, considered as background for the remote coastal station of Finokalia, a bimodal size distribution was found (Fig. 4a).

During these cases the Aitken and the accumulation modes were well distinguished, and the aerosol loading in both modes was low to moderate. An additional characteristic of these cases was that the Young Aitken mode included only a small fraction of the total particle number. When local/regional sources or long range transported air masses influenced the area, then pollution particles were superimposed on the background bimodal distribution. The result was a unimodal size distribution (Fig. 4b) in the accumulation mode range with high aerosol loading (notice the different colour scale

ACPD
8, 6571–6601, 2008

in the two graphs). A very interesting phenomenon is evidenced in Fig. 4b. Between 12:00 and 20:00 LT particles below 40 nm vanished and then appeared again. This phenomenon has been observed several times during the two month measurement period and is explicitly investigated in Sect. 4.

For a more detailed investigation of typical characteristics of the measured particle number size distributions, average distributions have been calculated for periods A, B and C, considered as representative distributions of maritime, polluted and mixed conditions (Fig. 5). Log-normal distributions have then been fitted and average geometric median diameters and standard deviations were extracted. In the case of maritime/background air masses (period A) the Aitken and the accumulation mode peak diameters were found at 66 and 195 nm, respectively, while during period C the influence from anthropogenic sources was seen as an enhancement of the Aitken mode towards peak diameters of somewhat finer particles (53 nm). During period B (polluted air masses) the average typically observed unimodal size distribution was centered around 139 nm.

3.2.2 New particle formation

The particle number size distributions during the ARIADNE field experiment was screened for possible events of secondary particle formation. The formation of new particles from gaseous precursors represents a major source of particle number (Kulmala et al., 2004), and it was not clear before our observations whether this phenomenon would happen in the East Mediterranean region frequently.

Owing to the lower size limit of our DMPS system, a particle formation event was defined as a period when high concentrations of particles occurred in the smallest size interval (18–25 nm). Between 29 August and 20 October 2005, only three new particle formation events were observed at Finokalia. These three cases met the criteria given in Birmili et al. (2003) to qualify as a significant particle formation event. The time for the Young Aitken curve to rise from 1/e of maximum to maximum value was between 0.5 and 1 h, and similar values were found for the declining branch. Maximum num-

ber concentrations <50 nm ranged between 1400–2400 cm^{-3}, which corresponded to 40–55% of the total particle number concentration. Formation rates determined by dividing the concentration of new particles formed by the time necessary to reach the concentration maximum yielded values between 1.1 and 1.7 $cm^{-3}\,s^{-1}$.

Figure 6 presents one of the three particle formation events, starting on 23 September at 11:00 LT. The occurrence of small particles (<50 nm) is limited to under two hours. This observation suggests that the particle formation took place in a small cell of the atmosphere only. All events observed during our experiment occurred during midday, suggesting that photochemical processes play key role. For all events the pre-event concentration of particles remained below 1200 cm^{-3}. Back trajectory analysis showed that during new particle formation events western winds prevailed in the area with the air masses originating from continental Europe.

It is an important observation that despite the large amounts of solar radiation encountered almost every day in the cloudless atmosphere over Crete, we recorded no large-area nucleation and growth events that are rather typical for the continental boundary layer (e.g. Kulmala et al., 2004; Heintzenberg et al., 2007). It remains a current subject of speculation why this is so. Reasons could be the lack of aerosol precursors, the scavenging of precursors by a large particle surface area in a regime of high relative humidity, or the lack of a vertical atmospheric exchange that is necessary to lift precursors to higher levels where temperatures are low and thus favourable for particle nucleation.

3.3 Apparent particle density and mass closure consideration

Assuming that PM_{10} measured corresponds to dry mass, we estimated PM_1 mass using the SDI mass size distributions. Then dividing PM_1 to dry volume we estimated the range of apparent densities and then discussed how realistic these densities are, based on the chemical composition where the dry mass is equally distributed to organic carbon and sulfate.

ACPD
8, 6571–6601, 2008

Particle number concentrations measured by electromobility analysis are based on the electromobility diameter which, after the elimination of multiple charge effects, is the particles' Stokes' diameter. The calculation of a particle mass, which can directly be compared to gravimetric measurements, requires assumption for particle shape and particle density. Particle volume concentrations were additionally calculated from number size concentrations assuming spherical particles. Volume concentrations were calculated separately for the fine and the coarse modes (1 μm cut off), and are plotted together with the PM_{10} mass concentration at Finokalia station for the same period (Fig. 7). Here, it is evident that the fine aerosol fraction controlled by far the variability of the total particle mass concentrations.

The derived volume concentrations were used in conjunction with continuous measurements of PM_{10} mass to estimate an apparent particle density. This was calculated only for the fine aerosol fraction, since the number concentration of coarse particles was very low, inducing significant errors in the coarse particle volumes, consequently leading to non-realistic densities. For the estimation of the PM_1 mass concentrations needed for the calculation of the apparent density of fine particles, PM_1/PM_{10} ratios from impactor measurements were accommodated (Gerasopoulos et al., 2007). For the days with impactor samples, a PM_1 time series was reconstructed from the PM_{10} data set in Fig. 7, assuming a constant PM_1/PM_{10} ratio during each 2–3 day sampling period.

Within ARIADNE, nine impactor samples were available and the apparent fine particle densities are shown in Fig. 8. In all cases, median densities ranged between 1–1.7 g cm^{-3}. Considering that the main part of the fine particle mode consisted of ammonium sulfate (Sciare et al., 2005), which has a density of ρ=1.75 g cm^{-3} (Lide, 1991), and organic matter assuming here a density of ρ=1.2 g cm^{-3} (Turpin and Lim, 2001), the calculated values were within a range of realistic densities for fine particles. Although chemical composition measurements are available, a direct comparison is not easy due to the numerous assumptions made in the calculations.

ACPD
8, 6571–6601, 2008

4 Disappearing Aitken particles: observations and model simulations

4.1 Systematic disappearance of Aitken particles

The systematic disappearance, or depletion of Aitken particles with diameters below 50 nm was observed at Finokalia station as a reoccurring feature. Example for this behavior are pictured in Figs. 6, 9a and 10a. As can be seen in Fig. 9a, this disappearance of Aitken particles took place gradually over hours, so that it is unlikely that it can be explained by air mass changes that involve rather abrupt changes in concentration. The disappearance was identified at almost half of all days, and its special pattern highly differed case by case.

Two patterns of Young Aitken particles depletion have been observed. The first pattern is characterized by a gradual depletion of the particles. In general, this pattern is not necessarily related to diurnal variation of solar irradiance, as its initiation appeared in the late afternoon or even before sunrise. The second pattern occurred only during day time and the maximum depletion was observed at noon or in the early afternoon while the depletion rate was more rapid. Both the depletion intensity and the frequency of the Aitken mode depletion events, decreased from summer to winter (not shown here), indicating that they were strongly dependent on solar irradiance variation and its impacts. The main mechanism driving this process is suspected to be either condensation of gas phase species onto small particles or coagulation processes. In order to study the impact of such a process, simulations of H_2SO_4 condensation on the measured distributions and self-coagulation within the existing particle number size distribution were performed.

4.2 Model description

A simplistic aerosol dynamics box model was applied to simulate the potential effects of coagulation and condensation on the particle number size distribution. The objective was not to achieve a full microphysical description of aerosol dynamical processes –

this would require the implementation of gas phase chemical reactions, mass transfer rates, chemical reactions within the particle as well as heterogeneous chemical reactions, but rather a plausibility check whether condensation and coagulation played a substantial role in the observed diurnal cycle of Aitken mode concentrations.

The submicrometer particle population was described by a sectional aerosol model. Experimental particle number size distributions served as the initial input of the model. Two processes were allowed to modify the particle number size distribution, condensation of sulfuric acid and self-coagulation. Condensation of condensable species will cause a growth of individual particles and process the particle number size distribution. Since condensation in the transition regime causes a growth of all particles by a similar diameter increment, condensation was accounted for by moving the sections of the aerosol model. As sulphuric acid (H_2SO_4) was assumed as the only condensable species, condensational growth was governed by the diffusion of sulphuric acid monomers. Mass transfer rates were calculated assuming spherical particles, a mass accommodation coefficient α of unity, and Dahneke's interpolation formula for vapour diffusion in the transition regime (Seinfeld and Pandis, 1998). Immediate neutralization with ammonia was assumed to take place, forming particulate ammonium sulphate.

H_2SO_4 concentrations were calculated from a simple chemical mass balance model considering production via the reaction of OH and SO_2, and the loss onto pre-existing aerosol (i.e. the condensational sink term CS) by using a pseudo-steady state approximation (e.g. Weber et al., 1997):

$$k \cdot [SO_2][OH] = [H_2SO_4] \cdot CS \quad (1)$$

with k=8.5×10^{13} cm^3 s^{-1} (DeMore et al., 1997). The diurnal cycle of OH was assumed to closely follow that of solar radiation. A general mean diurnal cycle with a peak value of 2×10^7 cm^{-3} was assumed for this study, based on earlier work at Finokalia (Berresheim et al., 2003). As shown in previous studies for the Mediterranean atmosphere, the simplistic mass balance approach was able to reproduce H_2SO_4 concentrations with a measure of determination R^2=0.86 (Bardouki et al., 2003; Mihalopoulos

ACPD
8, 6571–6601, 2008

et al., 1997).

The coagulation losses of particle number size concentration were calculated using the Dahneke kernel for particle diffusion in the transition regime (Seinfeld and Pandis, 1998). Since the size distribution change of low-concentration polydisperse aerosol populations is predominantly located in the size range below 100 nm, our aerosol model only accounted for coagulation losses of smaller particles onto bigger particles. In fact, no gain in particle diameter of larger particles was considered, thereby avoiding the need to numerically treat the complicated transition of larger particles from one to another size bin.

On any account, several limitations of the model need to be kept in mind during the discussion of the simulation results: The absence of condensable species beyond H_2SO_4 (this limitation is thought to be critical only for species with a diurnal cycle different from that of solar radiation), no new particle formation was considered during the mid-day observation period (i.e. only the existing size distribution is allowed to evolve with time), the requirement of a quasi Lagrangean observation, i.e. no significant air mass changes were accounted for during the simulation period.

4.3 Comparison between model results and observations

Two case studies were chosen to model the depletion of young Aitken particles. The aim was to explore impacts of variable precursor concentrations and condensational growth of the particle population and compare the results with observed number size distributions. Consecutive runs assuming different levels of H_2SO_4 were performed in order to estimate the total amount of vapors required to simulate the observed depletion of Young Aitken mode particles. In both cases best coherence was achieved using peak values for sulfuric acid of $1–2\times10^7$ molecules cm^{-3}. The above mentioned values are representative for the site of Finokalia station (Bardouki et al., 2003). Dry particle density was assumed to be 1.6 g cm^{-3} based on chemical analysis results for the investigated period, while wet particle growth factor was assumed 1.15. Sensitivity tests showed no temperature dependence in the range 283 K to 313 K, which is

ACPD
8, 6571–6601, 2008

representative for the temperatures recorded during this study.

The first case study corresponds to the event of 7 October 2005 and is representative of the first pattern (gradual depletion). As shown in Fig. 9a the depletion of Young Aitken particles began around 08:00 LT and lasted for about 10 h. The simulated condensation process (Fig. 9b) agrees well in both pattern and the depletion diameter cut off of 30 nm. Within the entire run, the bimodal distribution and the convergence of the two modes to one, at the end of the run, are well simulated. The modelled and observed total particle number concentrations, corresponding to the value at the end of the run, coincide within 7%, ensuring the stability of the air mass and the validity of the comparison made.

The second case of 15 October 2005 is characteristic of the second pattern described above (Fig. 10). In particular, an abrupt depletion was observed after 11:00 LT with a total duration of about 6 h (Fig. 10a). The observed depletion diameter cut off is 40 nm and is well captured by the model. The enhanced Aitken mode values after 14:00 LT are simulated in the model and the evolution of the distribution follows in general the nature of the measurement (Fig. 10b). The agreement between the modelled and observed total particle number concentrations at the final stage of the run is about 30%, possibly indicating inflow of accumulation mode particles.

Although the approach followed is simplistic, we were able to reproduce the time scale and the intensity of the phenomenon of depletion of Aitken mode particles, as well as the evolution of the particle number size distribution. An important conclusion hereof is that the formation of particles <50 nm seems to be absent despite the large amounts of solar radiation observed.

5 Conclusions

An intensive field study was conducted at the environmental research station Finokalia of the University of Crete, Greece, in order to better understand the variability and climatic relevance of atmospheric particles in the Eastern Mediterranean. The average

total particle number concentration (Diameter >18 nm) was found to be 1800 cm^{-3} with values ranging between 360 cm^{-3} and 4560 cm^{-3}. On average, half of the total particle concentration was assigned to accumulation mode (100–1000 nm), one third to the Aitken mode (50–100 nm) and the rest to the Young Aitken particles (18–50 nm). Coarse particles (1–10 μm) were limited in number throughout the measuring period but they could significantly contribute to the total particle volume (up to 30%) and mass. Four periods were selected corresponding to distinct synoptic air masses types. Periods A and C represented maritime air masses featuring low to moderate particle concentrations (900–2000 cm^{-3}) while periods B and D represented air masses influenced by the European continent with elevated concentrations (1800–2900 cm^{-3}). Depending on the air mass origin two structures of particle number size distributions were confirmed: bimodal in background marine conditions (periods A and C), and unimodal in polluted continental air masses. Apparent particle density calculations were performed combining electromobility analysis and gravimetric techniques. Median densities for fine particles ranged between 1–1.7 g cm^{-3}, while mass closure between the two different techniques was satisfactorily achieved.

During the entire campaign, only three occasions of secondary new particle formation (observational diameter range 18–50 nm) were detected. The three events were short-lived observations, with a duration of less than two hours each, and featured particle formation rates 1.1–1.7 cm^{-3} s^{-1}. It is worth to note that no large-area particle nucleation and growth events that are typical for the continental boundary layer (Kulmala et al., 2004; Heintzenberg et al., 2007) were observed. It is currently unclear why the production of new particles in the Eastern Mediterranean atmosphere is suppressed, given its high potential of photochemical precursor production.

On almost every second day, the diurnal cycle of the particle size distribution featured a systematic disappearance (depletion) of Young Aitken particles. Two types of depletion were observed, a gradual one with in general low depletion rates and one with higher depletion rates which was observed only during daytime and correlated with solar radiation. We compared these observations with simplistic box model simulations

ACPD
8, 6571–6601, 2008

of the particle size distribution involving only condensation of H_2SO_4 and coagulation onto bigger particles. Despite the simplistic approach, the relative agreement of observations and simulations suggest that during the days of Aitken particle depletion, condensation and coagulation are the main factors shaping the evolving size distribution. The comparison adds up to the impression that nucleation of new particles is either insignificant over the Eastern Mediterranean, or that newly formed particles are rapidly scavenged before reaching the observational size limit of 18 nm.

Acknowledgements. This work was supported by the Greek State Scholarships Foundation and by the Atmospheric Composition Change – The European Network of Excellence (ACCENT). The data evaluation for this paper were conducted within the European Integrated project on Aerosol Cloud Climate and Air Quality Interactions (EUCAARI), coordinated by M. Kulmala. The authors also acknowledge the NOAA Air Resources Laboratory (ARL) for the provision of the HYSPLIT transport and dispersion model (http://www.arl.noaa.gov/ready/hysplit4.html) used in this publication.

References

Bardouki, H., Berresheim, H., Vrekoussis, M., Sciare, J., Kouvarakis, G., Oikonomou, K., Schneider, J., and Mihalopoulos, N.: Gaseous (DMS, MSA, SO2, H2SO4 and DMSO) and particulate (sulfate and methanesulfonate) sulfur species over the northeastern coast of Crete, Atmos. Chem. Phys., 3, 1871–1886, 2003, http://www.atmos-chem-phys.net/3/1871/2003/.

Berresheim, H., Plass-Dülmer, C., Elste, T., Mihalopoulos, N., and Rohrer, F.: OH in the coastal boundary layer of Crete during MINOS: Measurements and relationship with ozone photolysis, Atmos. Chem. Phys., 3, 639–649, 2003, http://www.atmos-chem-phys.net/3/639/2003/.

Birmili, W., Stratmann, F., and Wiedensohler, A.: Design of a DMA-Based Size Spectrometer for a Large Particle Size Range and Stable Operation, J. Aerosol Sci., 30, 549–553, 1999.

Birmili, W., Berresheim, H., Plass-Dülmer, C., Elste, T., Gilge, S., Wiedensohler, A., and Uhrner, U.: The Hohenpeissenberg aerosol formation experiment (HAFEX): a long-term study including sizeresolved aerosol, H2SO4, OH, and monoterpenes measurements, Atmos. Chem.

Phys., 3, 361–376, 2003, http://www.atmos-chem-phys.net/3/361/2003/.
DeMore, W. B., Sander, S. P., Golden, D. M., Hampson, R. F., Kurylo, M. J., Howard, C. J., Ravishankara, A. R., Kolb, C. E., and Molina, M. J.: Chemical kinetics and photochemical data for use in stratospheric modeling, Evaluation number 12, JPL Publ., 97-4, 1997.
Draxler, R. R. and Hess, G. D.: An overview of the HYSPLIT 4 modelling system for trajectories, dispersion and deposition, Aust. Meteorol. Mag., 47, 295–308, 1998.
Gerasopoulos, E., Koulouri, E., Kalivitis, N., Kouvarakis, G., Saarikoski, S., Makela, T., Hillamo, R., and Mihalopoulos, N.: Size-segregated mass distributions of aerosols over Eastern Mediterranean: seasonal variability and comparison with AERONET columnar size-distributions, Atmos. Chem. Phys., 7, 2551–2561, 2007, http://www.atmos-chem-phys.net/7/2551/2007/.
Gerasopoulos, E., Kouvarakis, G., Vrekoussis, M., Kanakidou, M., and Mihalopoulos, N.: Ozone variability in the marine boundary layer of the Eastern Mediterranean based on 7-year observations, J. Geophys. Res., 110, D15309, doi:10.1029/2005JD005991, 2005.
Haywood, J. and Boucher, O.: Estimates of the Direct and Indirect Radiative Forcing due to Tropospheric Aerosols: A Review, Rev. Geophys., 38, 513–543, 2000.
HEI Perspectives: Understanding the Health Effects of Components of the Particulate Matter Mix: Progress and Next Steps, Health Effects Institute, Cambridge, MA., USA, 2002.
Heintzenberg, J., Wehner, B., and Birmili, W.: "How to find bananas in the atmospheric aerosol": new approach for analyzing atmospheric nucleation and growth events, Tellus, B59(2), 273–282, 2007.
Kalivitis, N., Gerasopoulos, E., Vrekoussis, M., Kouvarakis, G., Kubilay, N., Hatzianastassiou, N., Vardavas, I., and Mihalopoulos, N.: Dust transport over the eastern Mediterranean derived from Total Ozone Mapping Spectrometer, Aerosol Robotic Network, and surface measurements, J. Geophys. Res., 112, D03202, doi:10.1029/2006JD007510, 2007.
Kulmala, M., Vehkamäki, H., Petäjä, T., Dal Maso, M., Lauri, A., Kerminen, V.-M., Birmili, W., and McMurry, P. H.: Formation and growth rates of ultrafine atmospheric particles: a review of observations, J. Aerosol Sci., 35, 143–176, 2004.
Lelieveld, J., Berresheim H., Borrmann, S., Crutzen, P. J., Dentener, F. J., Fischer, H., Feichter, J., Flatau, P. J., Heland, J., Holzinger, R., Korrmann, R., Lawrence, M. G., Levin, Z., Markowicz, K. M., Mihalopoulos, N., Minikin, A., Ramanathan, V., de Reus, M., Roelofs, G. J., Scheeren, H. A., Sciare, J., Schlager, H., Schultz, M., Siegmund, P., Steil, B., Stephanou,

E. G., Stier, P., Traub, M., Warneke, C., Williams, J., and Ziereis, H.: Global air pollution crossroads over the Mediterranean, Science, 298, 794–799, 2002.
Lide, D. R.: CRC Handbook of Chemistry and Physics, CRC Press Inc, USA, 1991.
Lohmann, U. and Feichter, J.: Global indirect aerosol effects: a review, Atmos. Chem. Phys., 5, 715–737, 2005, http://www.atmos-chem-phys.net/5/715/2005/.
Maenhaut, W., Hillamo, R., Makela, T., Jafferzo, J.-L., Bergin, M. H., and Davidson, C. I.: A new cascade impactor for aerosol sampling with subsequent PIXE analysis, Nucl. Inst. & Meth. in Phys. Res., 109/110, 482–487, 1996.
Markowicz, K. M., Flatau, P. J., Ramana, M. V., Crutzen, P. J., and Ramanathan, V.: Absorbing Mediterranean aerosols lead to a large reduction in the solar radiation at the surface, Geophys.Res. Lett., 29(20), 1968, doi:10.1029/2002GL015767, 2002.
Mihalopoulos, N., Stephanou, E., Kanakidou, M., Pilitsidis, S., and Bousquet, P.: Tropospheric aerosol ionic composition above the eastern Mediterranean area, Tellus, 49B, 314–326, 1997.
Penner, J. E., Chuang, C. C., and Grant, K.: Climate forcing by carbonaceous and sulfate aerosols, Clim. Dynam., 14(12), 839–852, 1998.
Peters, T. M. and Leith, D.: Concentration measurement and counting efficiency of the aerodynamic particle sizer 3321, J. Aerosol Sci., 34, 627–634, 2003.
Petäjä, T., Kerminen, V.-M., Dal Maso, M., Junninen, H., Koponen, I. K., Hussein, T., Aalto, P. P., Andronopoulos, S., Robin, D., Hämeri, K., Bartzis, J. G., and Kulmala, M.: Sub-micron atmospheric aerosols in the surroundings of Marseille and Athens: physical characterization and new particle formation, Atmos. Chem. Phys., 7, 2705–2720, 2007, http://www.atmos-chem-phys.net/7/2705/2007/.
Ravishankara, A. R.: Heterogeneous and Multiphase Chemistry in the Troposphere, Science, 276, 1058–1065, 1997.
Sciare, J., Oikonomou, K., Cachier, H., Mihalopoulos, N., Andreae, M. O., Maenhaut, W., and Sarda-Esteve, R.: Aerosol mass closure and reconstruction of the light scattering coefficient over the Eastern Mediterranean Sea during the MINOS campaign, Atmos. Chem. Phys., 5, 2253–2265, 2005, http://www.atmos-chem-phys.net/5/2253/2005/.
Seinfeld, J. H. and Pandis, S. P.: Atmospheric Chemistry and Physics, 2nd Edition, John Wiley, New York, USA, 1998.

Solomon, S., Qin, D., Manning, M., Chen, Z., Marquis, M., Averyt, K. B., Tignor, M., and Miller, H. L.: Climate Change 2007: The Physical Science Basis, IPCC, contribution of Working Group I to the Fourth Assessment Report of the Intergovernmental Panel on Climate Change (IPCC), Cambridge Univ. Press, Cambridge, United Kingdom, 2007.

Turpin, B. J. and Lim, H.-J.: Species Contributions to PM2.5 Mass Concentrations: Revisiting Common Assumptions for Estimating Organic Mass, Aerosol Sci. Technol., 35, 602–610, 2001.

Vrekoussis, M., Liakakou, E., Kocak, M., Kubilay, N., Oikonomou, K., Sciare, J., and Mihalopoulos, N.: Seasonal variability of optical properties of aerosols in the Eastern Mediterranean, Atmos. Environ., 39, 7083–7094, 2005.

Weber, R. J., Marti, J. J.,McMurry, P. H., Eisele, F. L., Tanner, D. J., and Jefferson, A.: Measurement of new particle formation and ultrafine particle growth rates at a clean continental site, J. Geophys. Res. 102, 4375–4385, 1997.

Winklmayr, W., Reischl, G. P., Linde, A. O., and Berner, A.: A New Electromobility Spectrometer For the Measurement of Aerosol Size Distributions in the Size Range from 1 to 1000 nm, J. Aerosol Sci., 22, 289–296, 1991.

WHO: Health Effects of Air Pollution Results from the WHO Project: "Systematic Review of Health Aspects of Air Pollution in Europe", World Health Organisation, Geneva, Switzerland, 2004.

Table 1. Classification of four distinct air masses and their corresponding total particle number concentration (Diameter >18 nm).

Period	Duration	Particle Type	Number Concentration (cm^{-3})
A	21 Sep 2005 10:30–25 Sep 2005 00:00	Marine	900–1200
B	27 Sep 2005 18:00–30 Sep 2005 18:00	Polluted	2300–2900
C	1 Oct 2005 22:00–4 Oct 2005 10:00	Marine (mixed)	1200–2000
D	5 Oct 2005 00:00–12 Oct 2005 00:00	Polluted	1800–2500

ACPD
8, 6571–6601, 2008

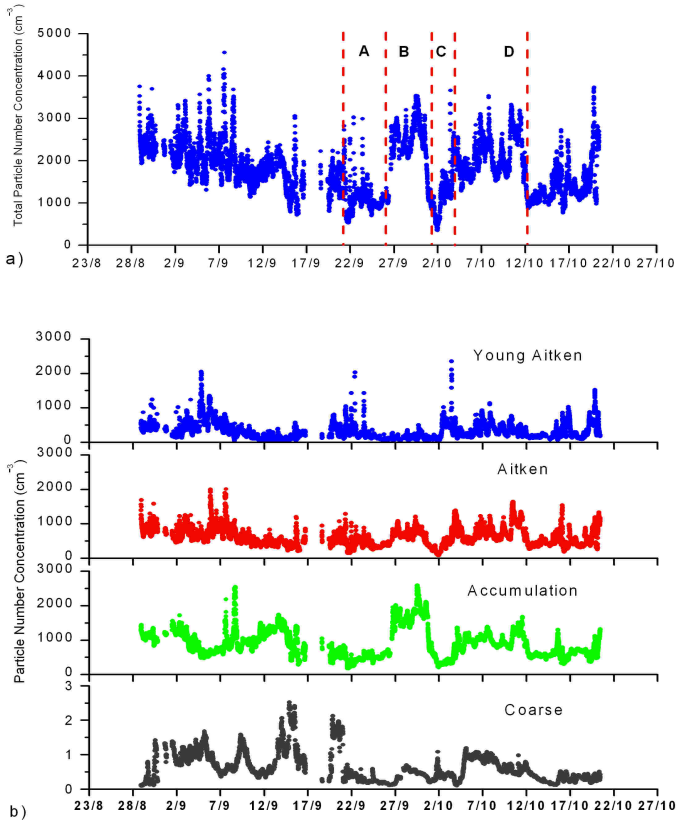

Fig. 1. Particle concentrations at Finokalia, Crete between 28 August and 20 October 2005: **(a)** total number (>18 nm), **(b)** Young Aitken (18–50 nm), Aitken (50–100 nm), accumulation (100–1000 nm) and coarse (1–10 μm) particle concentrations. Periods A, B, C and D are defined in Table 1.

ACPD
8, 6571–6601, 2008

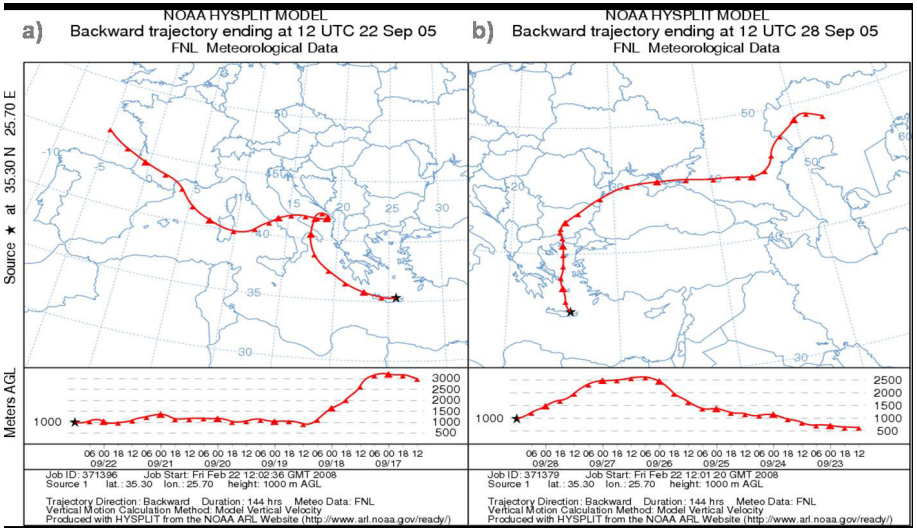

Fig. 2. Representative back trajectories illustrating **(a)** Maritime air masses corresponding to Period A , **(b)** Polluted air masses corresponding to Period B.

ACPD
8, 6571–6601, 2008

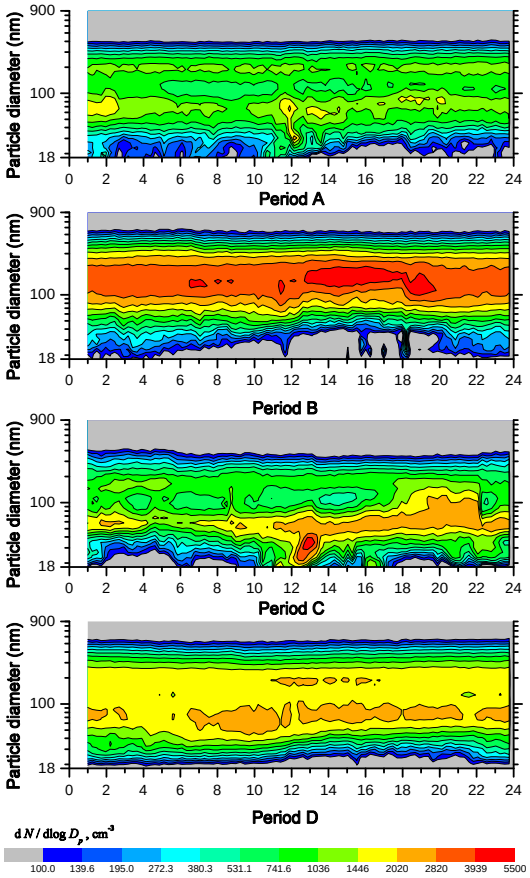

Fig. 3. Average diurnal cycle of the particle number size distributions during the four periods defined in Table 1.

ACPD
8, 6571–6601, 2008

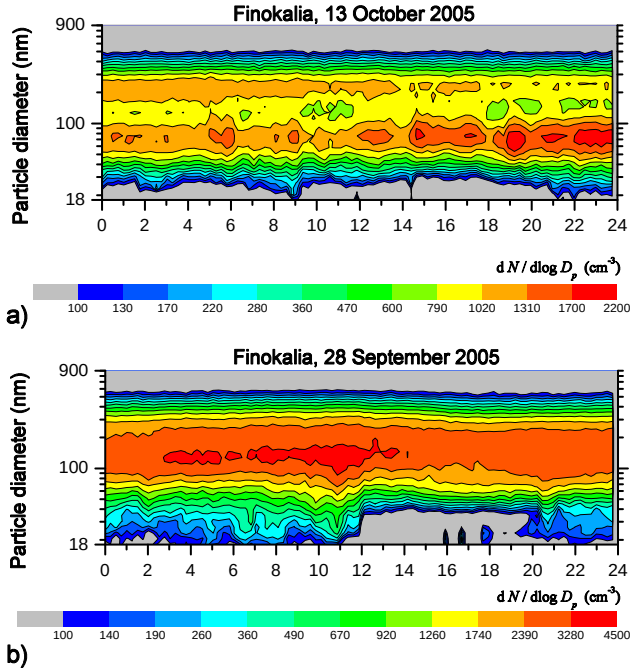

Fig. 4. Extreme cases of particle number size distributions during the influence of **(a)** maritime air and **(b)** polluted continental air.

ACPD
8, 6571–6601, 2008

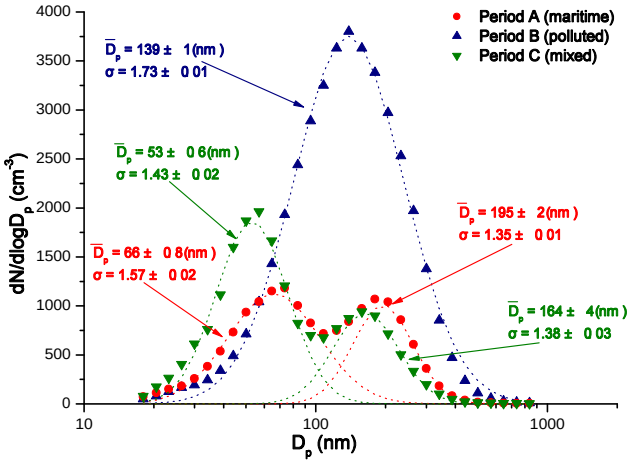

Fig. 5. Particle number size distributions representing different degrees of anthropogenic influence: Air masses A, B and C defined in Table 1.

ACPD
8, 6571–6601, 2008

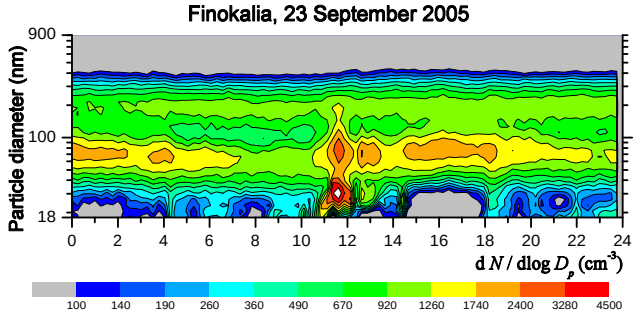

Fig. 6. New particle formation event observed on 23 September 2005 at Finokalia.

ACPD
8, 6571–6601, 2008

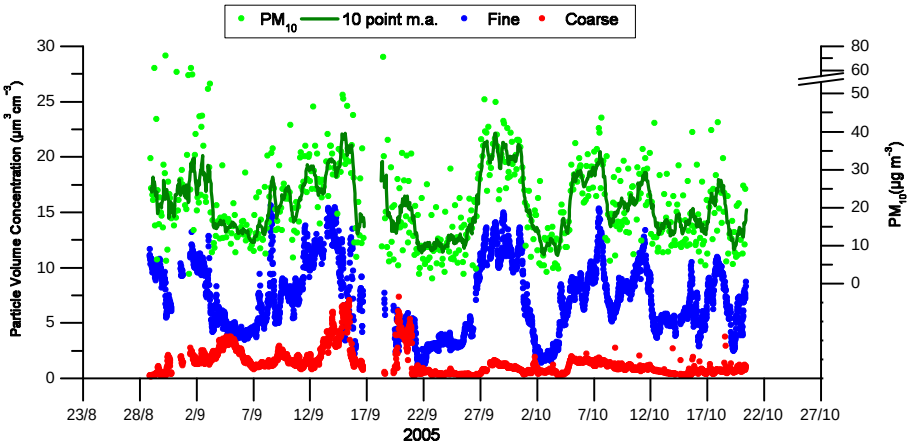

Fig. 7. Fine (<1 μm) and coarse (>1 μm) particle volume concentrations as well as PM_{10} mass concentration at Finokalia station.

ACPD
8, 6571–6601, 2008

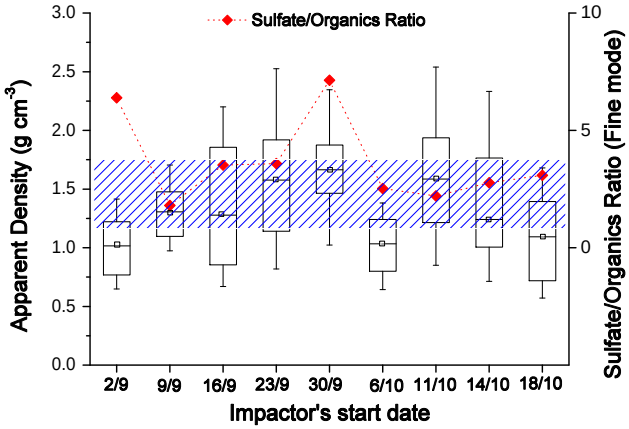

Fig. 8. Apparent fine particle density at Finokalia. Calculations were made assuming a constant PM_1/PM_{10} ratio during each sampling period.

ACPD
8, 6571–6601, 2008

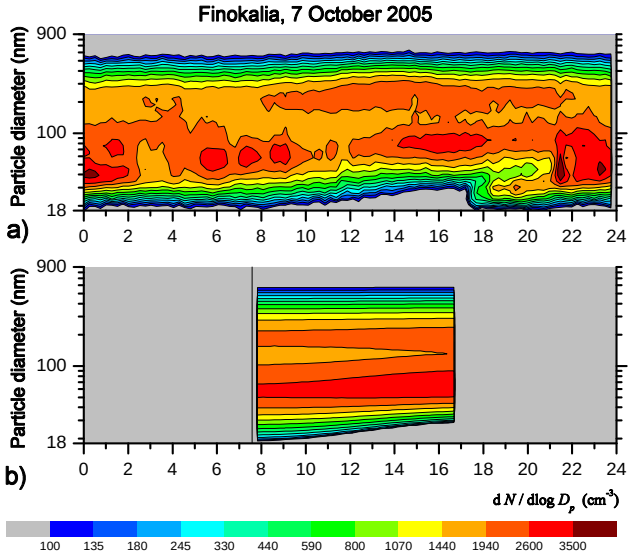

Fig. 9. Particle number size distributions at Finokalia on 7 October 2005: **(a)** Measurement illustrating the gradual disappearance of Aitken mode particles, **(b)** box model simulation starting at 08:00 LT and involving only condensation and particle coagulation.

ACPD
8, 6571–6601, 2008

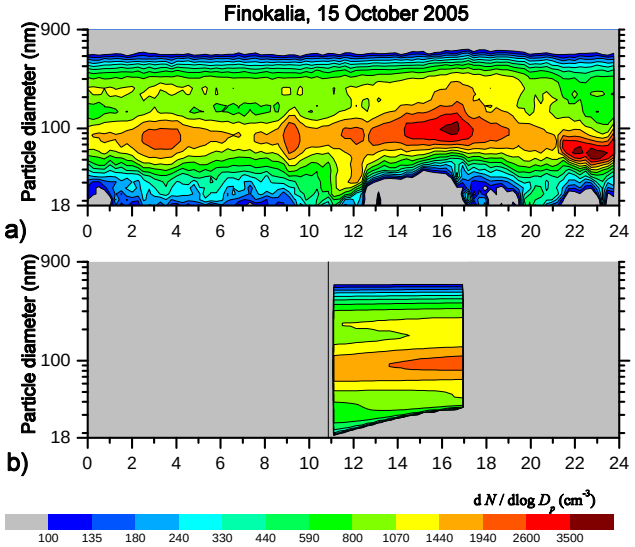

Fig. 10. Particle number size distributions at Finokalia on 15 October 2005: **(a)** Measurement illustrating a rather abrupt disappearance of Aitken mode particles during mid-day, **(b)** box model simulation starting at 11:00 LT and involving only condensation and particle coagulation.

ACPD
8, 6571–6601, 2008